

## Article

# Improving of Thermoelectric Efficiency of Layered Sodium Cobaltite Through Its Doping by Different Metal Oxides

Natalie S. Krasutskaya <sup>1</sup>, Ekaterina A. Chizhova <sup>1</sup>, Julia A. Zizika <sup>2</sup>, Alexey V. Buka <sup>3</sup>, Hongchao Wang <sup>4</sup> and Andrei I. Klyndyuk <sup>1,5,\*</sup>

<sup>1</sup> Department of Physical, Colloid and Analytical Chemistry, Organic Substances Technology Faculty, Belarusian State Technological University, Sverdlova Str. 13a, 220006 Minsk, Belarus; krasutskaya@belstu.by (N.S.K.); chizhova@belstu.by (E.A.C.)

<sup>2</sup> Structural Analysis Sector, Physical-Technical Institute of the National Academy of Science of Belarus, Academician Kuprevich Str. 10, 220084 Minsk, Belarus; egorova.y\_a@mail.ru

<sup>3</sup> Department of Glass, Ceramics and Binding Materials Technology, Chemical Technology and Engineering Faculty, Belarusian State Technological University, Sverdlova Str. 13a, 220006 Minsk, Belarus; lesa\_buka@hotmail.com

<sup>4</sup> School of Physics, State Key Laboratory of Crystal Materials, Shandong University, Jinan 250100, China; wanghc@sdu.edu.cn

<sup>5</sup> Department of Physical Chemistry and Electrochemistry, Chemical Faculty, Belarusian State University, Nezavisimosti Av. 4, 220030 Minsk, Belarus

\* Correspondence: klyndyuk@belstu.by; Tel.: +375-(29)-6365624

## Abstract

$\text{Na}_{0.89}\text{Co}_{0.90}\text{Me}_{0.10}\text{O}_2$  (Me = Cr, Ni, Mo, W, Pb, and Bi) ceramic samples were prepared using a solid-state reaction method, and their crystal structure, microstructure, and electrical, thermal, and thermoelectric properties were investigated. The effect of the nature of the doping metal (Me = Cr, Ni, Mo, W, and Bi) on the structure and properties of layered sodium cobaltite  $\text{Na}_{0.89}\text{CoO}_2$  was analyzed. The largest Seebeck coefficient (616  $\mu\text{V}/\text{K}$  at 1073 K) and figure-of-merit (1.74 at 1073 K) values among the samples studied were demonstrated by the  $\text{Na}_{0.89}\text{Co}_{0.9}\text{Bi}_{0.1}\text{O}_2$  solid solution, which was also characterized by the lowest value of the dimensionless relative self-compatibility factor of about 8% within the 673–873 K temperature range. The obtained results demonstrate that doping of layered sodium cobaltite by transition and heavy metal oxides improves its microstructure and thermoelectric properties, which shows the prospectiveness of the used doping strategy for the development of new thermoelectric oxides with enhanced thermoelectric characteristics. It was also shown that samples with a higher sodium content (Na:Co = 0.89:1) possessed higher chemical and thermal stability than those with a lower sodium content (Na:Co = 0.55:1), which makes them more suitable for practical applications.

**Keywords:** thermoelectric oxides; layered sodium cobaltite; microstructure; electrical properties; thermal properties; figure-of-merit



Academic Editor: Gilbert Fantozzi

Received: 8 May 2025

Revised: 19 June 2025

Accepted: 1 July 2025

Published: 5 July 2025

**Citation:** Krasutskaya, N.S.; Chizhova, E.A.; Zizika, J.A.; Buka, A.V.; Wang, H.; Klyndyuk, A.I.

Improving of Thermoelectric Efficiency of Layered Sodium Cobaltite Through Its Doping by Different Metal Oxides. *Ceramics* **2025**, *8*, 86. <https://doi.org/10.3390/ceramics8030086>

**Copyright:** © 2025 by the authors. Licensee MDPI, Basel, Switzerland. This article is an open access article distributed under the terms and conditions of the Creative Commons Attribution (CC BY) license (<https://creativecommons.org/licenses/by/4.0/>).

## 1. Introduction

Approximately two-thirds of the energy consumed by factories, transport, and households is dissipated into the environment and, in fact, lost for humanity [1]. This high-potential waste heat can be partially converted into electrical energy using thermoelectrogenerators (TEGs). To produce TEGs, one needs so-called thermoelectric materials, which should possess a complex of unique properties, such as low electrical resistivity ( $\rho$ ) and

thermal conductivity ( $\lambda$ ), high values of Seebeck coefficient ( $S$ ), etc. [2–5]. Traditional thermoelectrics based on layered chalcogenides of bismuth and lead possess several drawbacks, including the presence of toxic, rare, and expensive components, as well as instability in air at elevated temperatures. These drawbacks are absent for oxide thermoelectrics [6–10]. One of the well-known representatives of them is layered sodium cobaltite  $\text{Na}_x\text{CoO}_2$ , first described by Jansen and Hoppe [11] and characterized as thermoelectric by Terasaki et al. [12]. Its structure consists of  $[\text{CoO}_2]$  layers (CdI<sub>2</sub> structure) with sodium atoms in between [13]. According to Viciu et al. [14], the concentration of oxygen vacancies in the  $[\text{CoO}_2]$  layers is negligible; therefore, the oxidation state of cobalt ions is determined only by the sodium content ( $x_{\text{Na}}$ ). Due to its unique transport properties,  $\text{Na}_x\text{CoO}_2$  is considered as potential material for  $p$ -branches of TEGs and ceramic (oxide) thermocouples [15,16], cathode material of sodium-ion batteries (SIBs) [17–20], and its crystal hydrate,  $\text{Na}_x\text{CoO}_2 \cdot y\text{H}_2\text{O}$ , below 4 K undergoes into a superconducting state [21]. The crystal structure, electrotransport, thermal, and functional characteristics of  $\text{Na}_x\text{CoO}_2$  strongly depend on the sodium content [22–25].

The functional characteristics of the ceramic samples of the layered sodium cobaltite are worse than those of monocrystals; however, they can be improved using different approaches: (i) doping in sublattices of cobalt [26–28] or/and sodium [29–31], (ii) modification by particles of metals [32,33] or semiconductors [34], (iii) using so-called soft synthesis methods [7,35,36], and (iv) using special sintering techniques [37], resulting in the improvement of the ceramic microstructure which enhances its electrotransport and mechanical properties.

Partial substitution of cobalt by copper in  $\text{NaCo}_{2-x}\text{Cu}_x\text{O}_4$  ceramics improves its sinterability, lowers electrical resistivity and enhances Seebeck coefficient, resulting in essential increase of power factor values of these solid solutions comparing to the unsubstituted sodium cobaltite [38,39], which reaches maximal value for  $\text{NaCo}_{1.8}\text{Cu}_{0.2}\text{O}_4$  phase—3.08 mW/(m·K<sup>2</sup>) at 1073 K [38]. Substitution of cobalt by nickel deteriorates sinterability of  $\text{NaCo}_{2-x}\text{Ni}_x\text{O}_4$  phases, but decreases their  $\rho$  and strongly enlarges  $S$ , and  $p$  value for  $\text{NaCo}_{1.9}\text{Ni}_{0.1}\text{O}_4$  at 1073 K reaches 2.36 mW/(m·K<sup>2</sup>), which is 8 times larger than for the base  $\text{NaCo}_2\text{O}_4$  phase [40,41]. When zinc substitutes cobalt in  $\text{NaCo}_{2-x}\text{Zn}_x\text{O}_4$ , the electrical resistivity and Seebeck coefficient of ceramics increase, and the power factor reaches 1.7 mW/(m·K<sup>2</sup>) at 1073 K for  $\text{NaCo}_{1.9}\text{Zn}_{0.1}\text{O}_4$  solid solution, which is 4 times larger than for  $\text{NaCo}_2\text{O}_4$  cobaltite [42]. Co-substitution of Na by Bi and Co by Mn in  $\text{Na}_{0.81}\text{CoO}_2$  decreases its  $\rho$  and increases its  $S$ , which results in a strong increase in the  $p$  values of ceramics, reaching 0.632 mW/(m·K<sup>2</sup>) at 781 K for  $\text{Na}_{0.66}\text{Bi}_{0.15}\text{Co}_{0.99}\text{Mn}_{0.01}\text{O}_2$  compound, which is three times larger than that of the parent  $\text{Na}_{0.81}\text{CoO}_2$  phase [43].

The authors of [44] produced a  $\pi$ -shaped thermoelectric device consisting of  $\text{Na}_{0.50}\text{Co}_{0.85}\text{Cu}_{0.15}\text{O}_2$  ( $p$ -leg) cobaltite and  $\text{Ba}_{0.2}\text{Sr}_{0.8}\text{PbO}_3$  ( $n$ -leg) plumbate, which produced an output power of 12 mW when the temperatures of the hot and cold sides were 1045 K and 539 K, respectively [44]. The power generation properties of this element did not change after high-temperature operation for seven days [44].

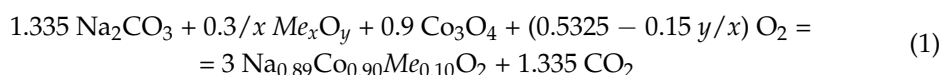
Earlier, we estimated the possibility of improving the thermoelectric performance of  $\text{Na}_x\text{CoO}_2$  by increasing the sodium content in it [25] and by doping sodium-poor  $\text{Na}_{0.55}\text{CoO}_2$  cobaltite with oxides of different transition and non-transition metals [16,45].

In this work, the effect of the nature of different transition or heavy metals partially substituting cobalt in the sodium-rich  $\text{Na}_{0.89}\text{CoO}_2$  layered cobaltite on its crystal structure, microstructure, thermophysical, electrophysical, and thermoelectric (functional) properties was studied. The chemical and thermal stabilities of the obtained materials were also studied and compared with those of sodium-poor  $\text{Na}_{0.55}\text{Co}_{0.90}\text{Me}_{0.10}\text{O}_2$  layered cobaltites [16]. It was found that the modification of  $\text{Na}_x\text{CoO}_2$  by different metal oxides, along with an

increase in sodium content from  $x = 0.55$  to  $x = 0.89$ , resulted in an essential enhancement of its thermoelectric performance and chemical and thermal stabilities. This led us to consider the materials obtained in this work as attractive for practical applications in thermoelectric devices for different purposes. To the best of our knowledge, such complex studies have not been performed earlier, and the results of this work bring new knowledge in the field of thermoelectric materials science compared to previously published works [16,25,28,29,36,37,45].

## 2. Materials and Methods

Ceramic samples of  $\text{Na}_{0.89}\text{Co}_{0.90}\text{Me}_{0.10}\text{O}_2$  ( $\text{Me} = \text{Cr}, \text{Ni}, \text{Mo}, \text{W}, \text{Pb}, \text{and Bi}$ ) were obtained using a solid-state reaction method according to the following reaction scheme:



The substitution level of 10 mol. % was chosen as for lower substitution degree it can be hard to detect the effect of substitution on the structure and properties of the parent phase, but for the higher substitution degrees the solubility level can be exceeded [38,40], which results in the formation of not single-phase but composite ceramics.

The dopants were selected, firstly, to provide neutral ( $\text{Cr}^{3+}$ ), acceptor ( $\text{Ni}^{2+}$ ), and donor ( $\text{Mo}^{6+}$ ,  $\text{W}^{6+}$ ,  $\text{Pb}^{4+}$ ,  $\text{Bi}^{5+}$ ) character of substitution without the size factor effect due to the slight difference in the ionic radii values of substituted ( $\text{Co}^{3+}$ ,  $\text{Co}^{4+}$  in  $\text{CoO}_6$  octahedra (C.N. = 6) of  $\text{Na}_x\text{CoO}_2$  crystal structure) and substituting ions [46], secondly, to use both transition (Cr, Ni) and heavy metals (W, Pb, Bi), and, thirdly, to demonstrate the effectiveness of some chosen dopants in enhancing the thermoelectric performance of layered sodium cobaltite [16,38–43].

The powders of  $\text{Na}_2\text{CO}_3$  (99%),  $\text{Co}_3\text{O}_4$  (99%),  $\text{Cr}_2\text{O}_3$  (99%),  $\text{NiO}$  (99.99%),  $\text{MoO}_3$  (99.99%),  $\text{WO}_3$  (99.99%),  $\text{PbO}$  (99.99%), and  $\text{Bi}_2\text{O}_3$  (99.99%) were taken in the ratio of  $\text{Na}:\text{Co}:\text{Me} = 1.2:0.9:0.1$  (the excess of  $\text{Na}_2\text{CO}_3$  in the initial mixture is taken to compensate for the loss of  $\text{Na}_2\text{O}$  from the samples during their thermal treatment and to obtain ceramics of the specified composition [25,46]). The powdered samples were milled in a planetary mill PM 100 Retsch (material of beakers and grinding balls— $\text{ZrO}_2$ ) for 90 min at 300 rpm with the addition of  $\text{C}_2\text{H}_5\text{OH}$  (~3–5 wt.%). The resulting slurries were air-dried at a temperature of 323 K and then pressed into tablets with a diameter of 19 mm and a thickness of up to 5 mm. Subsequently, the obtained samples were calcined in air for 12 h at a temperature of 1133 K. The calcination temperature of 1133 K was chosen to reduce the calcination time, as at this temperature, one of the initial reagents,  $\text{Na}_2\text{CO}_3$ , melts ( $T_m = 1127 \text{ K}$  [47]). Subsequently, after calcination, the blanks were ground in an agate mortar and re-milled in a planetary mill, then pressed into bars measuring  $5 \times 5 \times 30 \text{ mm}^3$  and tablets with a diameter of 15 mm and a thickness of 2–3 mm, which were sintered in air for 12 h at a temperature of 1203 K [46]. A sintering temperature of 1203 K was selected based on the results of previous studies [48], as at lower sintering temperatures, samples possessed high porosity values, and at higher sintering temperatures, they partially melted and reacted with the crucible material (alundum).

The real sodium content ( $x_{\text{Na}}$ ) and average oxidation state of cobalt ( $\text{Co}^{+Z}$ ) in the obtained ceramic materials were determined using iodometric [48] and reverse potentiometric titrations [49], as well as spectrophotometrically, according to the method described in [50] (see Supplementary Information).

The phase composition of the samples and the calculation of the crystal lattice parameters of the  $\text{Na}_{0.89}\text{Co}_{0.90}\text{Me}_{0.10}\text{O}_2$  layered cobaltites were performed by means of X-ray

diffraction analysis (XRD) using a Bruker D8 XRD Advance X-ray diffractometer (Bruker Optik GmbH, Ettlingen (Germany)) (CuK $\alpha$  radiation ( $\lambda = 1.5406 \text{ \AA}$ )).

The values of the coherent scattering area for the Na<sub>0.89</sub>Co<sub>0.90</sub>Me<sub>0.10</sub>O<sub>2</sub> ceramics were calculated using the Debye–Scherrer equation ( $D_S$ ) (2) [51] and size-strain method ( $D_{SS}$ ) (3) [52].

$$D_S = \frac{0.9 \cdot \lambda}{\beta \cdot \cos \Theta}, \quad (2)$$

$$(d \cdot \beta \cdot \cos \Theta) = \left( \frac{0.9 \cdot \lambda}{D_{SS}} \right) \cdot (d^2 \cdot \beta \cdot \cos \Theta) + \left( \frac{\varepsilon}{2} \right)^2, \quad (3)$$

where  $d$  is the interplanar distance (nm),  $\beta$  is the full width of the reflex at its half maxima (rad),  $\Theta$  is the diffraction angle ( $^\circ$ ), and  $\varepsilon$  is the microstrain.

The degree of crystallographic orientation of the grains of the Na<sub>0.89</sub>Co<sub>0.90</sub>Me<sub>0.10</sub>O<sub>2</sub> ceramics was evaluated using the Lotgering factor, as shown in Equation (4) [53]:

$$f = \frac{p - p_0}{1 - p_0}, \quad (4)$$

where  $p = \Sigma I(00l) / \Sigma I(hkl)$  ( $\Sigma I$  is the sum of the counts of X-ray diffraction peaks of the synthesized samples);  $p_0 = \Sigma I_0(00l) / \Sigma I_0(hkl)$  ( $\Sigma I_0$  is the sum of the counts of X-ray diffraction peaks of the reference phase JCPDC #00-030-1182).

The apparent density of the Na<sub>0.89</sub>Co<sub>0.90</sub>Me<sub>0.10</sub>O<sub>2</sub> ceramic samples ( $d_{EXP}$ ) was determined based on their mass and geometric dimensions, and their total porosity ( $\Pi_t$ ) was calculated using the following formula:

$$\Pi_t = \left( 1 - \frac{d_{EXP}}{d_{XRD}} \right) \cdot 100\%, \quad (5)$$

where  $d_{XRD}$  is the X-ray density of the sample ( $\text{g}/\text{cm}^3$ ).

The open porosity of the sintered samples ( $\Pi_o$ ) was determined by weighing the ceramic samples of Na<sub>0.89</sub>Co<sub>0.90</sub>Me<sub>0.10</sub>O<sub>2</sub>, which were saturated with ethyl acetate for 60 min under a vacuum of 25–30 Pa, and then weighed in ethyl acetate, according to Equation (6):

$$\Pi_o = \frac{m_1 - m}{m_1 - m_2} \cdot 100\%, \quad (6)$$

where  $m$  is the mass of the dry ceramic sample (g),  $m_1$  and  $m_2$  are the masses of the sample saturated with liquid ethyl acetate during weighing in air and that introduced into liquid ethyl acetate, respectively (g).

The microstructure and chemical composition of the Na<sub>0.89</sub>Co<sub>0.90</sub>Me<sub>0.10</sub>O<sub>2</sub> samples were studied using scanning electron microscopy (SEM) using a Tescan MIRA 3 LMH scanning electron microscope equipped with an AZtecLIVE Advanced energy dispersive microanalysis system with a nitrogen-free Ultim Max 100 standard detector (Oxford Instruments Analytical Ltd., High Wycombe (UK)).

The thermal expansion, electrical resistivity ( $\rho$ ), and Seebeck coefficient ( $S$ ) of the sintered ceramics were measured in air within a temperature range of 323–1073 K using the methodology described in [39,54,55]. The values of the average linear thermal expansion coefficient ( $\alpha$ , LTEC) were calculated from the linear parts of the  $\Delta l/l_0 = f(T)$  plots.

The thermal diffusivity ( $\eta$ ) of the Na<sub>0.89</sub>Co<sub>0.90</sub>Me<sub>0.10</sub>O<sub>2</sub> layered cobaltites was studied in a helium atmosphere over a temperature range of 323–1073 K using an LFA 457 Micro-Flash device (NETZSCH, Selb (Germany)). The thermal conductivity ( $\lambda$ ) of the Na<sub>0.89</sub>Co<sub>0.90</sub>Me<sub>0.10</sub>O<sub>2</sub> sintered ceramics was calculated using Equation (7).

$$\lambda = \eta \cdot d_{EXP} \cdot C_p, \quad (7)$$

where  $C_p$  is heat capacity, calculated by the Dulong–Petit law, (J/(g·K)). Thus, according to the data of works [16,56], the heat capacity of layered sodium cobaltite near 300 K becomes slightly dependent on the temperature and reaches a plateau.

The phonon ( $\lambda_{ph}$ ) and electron ( $\lambda_e$ ) parts of the thermal conductivity of the  $\text{Na}_{0.89}\text{Co}_{0.90}\text{Me}_{0.10}\text{O}_2$  ceramics were roughly approximated by Equations (8) and (9)

$$\lambda = \lambda_e + \lambda_{ph} \quad (8)$$

$$\lambda_e = \frac{L \cdot T}{\rho} \quad (9)$$

where  $L$  is the Lorentz number ( $L = 2.45 \times 10^{-8} \text{ W} \cdot \Omega \cdot \text{K}^{-2}$ ).

The values of the power factor ( $P$ ) and figure of merit ( $ZT$ ) of the  $\text{Na}_{0.89}\text{Co}_{0.90}\text{Me}_{0.10}\text{O}_2$  solid solutions were calculated using the following formula:

$$P = \frac{S^2}{\rho} \quad (10)$$

and

$$ZT = \frac{P \cdot T}{\lambda} \quad (11)$$

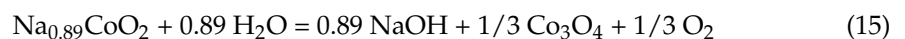
The self-compatibility factor ( $s$ ) and the dimensionless relative self-compatibility factor ( $\Delta s$ ) [57] for the  $\text{Na}_{0.89}\text{Co}_{0.90}\text{Me}_{0.10}\text{O}_2$  ceramics were calculated using Equations (12) and (13)

$$s = \frac{\sqrt{1 + ZT} - 1}{S \cdot T} \quad (12)$$

and

$$\Delta s = \frac{s_{max} - s_{min}}{s_{min}} \cdot 100\%. \quad (13)$$

The chemical stability of the  $\text{Na}_{0.89}\text{Co}_{0.90}\text{Me}_{0.10}\text{O}_2$  and  $\text{Na}_{0.55}\text{Co}_{0.90}\text{Me}_{0.10}\text{O}_2$  [16] samples to the impact of atmospheric water and carbon dioxide was estimated based on the results of their exposure for ten months in wet air at room temperature and a relative moisture of about 75% using optical microscopy (Levenhuk DTX 500 LCD (Levenhuk Inc., Praha (Czech Republic)), XRD (Bruker D8 XRD Advance X-ray diffractometer), infrared absorption spectroscopy (Thermo Nicolet Nexus ESP IR spectrometer (Nicolet Instrument Corporation, Madison (WI, USA))), and gravimetry (RADWAG AS/C/2/N 220 (Radwag Wagi Elektroniczne, Radom (Poland))). According to [16] and the results of XRD and IR-absorption spectroscopy, surface degradation of layered sodium cobaltite is described by Equations (14) and (15)



The intensity of chemical degradation of the samples in air was also estimated by comparing their electrotransport properties (electrical resistivity and Seebeck coefficient) before and after their storage in the measuring set within two weeks.

The thermal stability of the materials was estimated as their durability under operational conditions by comparing their electrical resistivity values after multiple thermocycles within the 323–1073 K temperature interval and after annealing in the measuring set within eight hours at 1073 K in air.

### 3. Results and Discussion

The sodium content in the obtained samples ( $x_{\text{Na}}$ ), determined by iodometry, reverse potentiometry, and spectrophotometry methods, was approximately 0.89 for all the investigated samples (Tables 1 and S1). The average oxidation state of cobalt in the  $\text{Na}_{0.89}\text{Co}_{0.90}\text{Me}_{0.10}\text{O}_2$  ( $\text{Me} = \text{Cr, Co, Ni, Mo, W, and Bi}$ ) layered cobaltites varied within 2.78–3.23 (Tables 1 and S1), increasing with the substitution of an acceptor character (Ni instead of Co) and decreasing with the substitution of a donor character (Mo, W, Pb, or Bi instead of Co), which was also observed for the  $\text{Na}_{0.55}\text{Co}_{0.90}\text{Me}_{0.10}\text{O}_2$  samples in a previous study [16]. Therefore, Co exists in the  $\text{Na}_{0.89}\text{Co}_{0.90}\text{Me}_{0.10}\text{O}_2$  compounds as a mixture of  $\text{Co}^{3+}$  and  $\text{Co}^{4+}$ ,  $\text{Co}^{2+}$  and  $\text{Co}^{3+}$ , and only  $\text{Co}^{3+}$  for  $\text{Me} = \text{Cr, Co, and Ni}$ ;  $\text{Me} = \text{Mo, W, and Bi}$ ; and  $\text{Me} = \text{Pb}$ .

**Table 1.** Values of sodium content ( $x_{\text{Na}}$ ), the average oxidation state of cobalt ( $\text{Co}^{+Z}$ ), lattice constants ( $a$ ,  $c$ ,  $c/a$ ,  $V$ ), Lotgering factor ( $f$ ), size of the coherent scattering area obtained using the Debye–Scherrer equation ( $D_s$ ) and the size-strain method ( $D_{\text{SS}}$ ), microstrain ( $\epsilon$ ) and X-ray density ( $d_{\text{XRD}}$ ) of  $\text{Na}_{0.89}\text{Co}_{0.9}\text{Me}_{0.1}\text{O}_2$  ( $\text{Me} = \text{Cr, Co, Ni, Mo, W, Pb, Bi}$ ) ceramic samples.

<i>Me</i>	$x_{\text{Na}}$	$\text{Co}^{+Z}$	$a$ , Å	$c$ , Å	$c/a$	$V$ , Å <sup>3</sup>	$f$	$D_s$ , nm	$D_{\text{SS}}$ , nm	$\epsilon \times 10^4$	$d_{\text{XRD}}$ , g/cm <sup>3</sup>
Cr	0.893	3.11	2.825	10.93	3.870	75.53	0.90	69	62	3.43	4.86
Co	0.891	3.11	2.826	10.94	3.872	75.71	0.31	63	45	4.56	4.98
Ni	0.889	3.23	2.831	10.92	3.856	75.75	0.69	70	70	2.61	4.88
Mo	0.894	2.78	2.822	10.96	3.883	75.57	0.87	73	70	1.41	5.06
W	0.889	2.78	2.825	10.97	3.884	75.80	0.92	67	69	1.50	5.43
Pb	0.888	3.01	2.825	10.94	3.873	75.64	0.92	79	60	3.22	5.55
Bi	0.894	2.90	2.823	10.93	3.872	75.45	0.76	77	72	2.49	5.56

According to the XRD results, all ceramic samples were single-phase within the XRD accuracy. The ceramic samples of  $\text{Na}_{0.89}\text{Co}_{0.90}\text{Me}_{0.10}\text{O}_2$  ( $\text{Me} = \text{Cr, Ni, Mo, W, Bi}$ ) obtained in this study, similar to the base  $\text{Na}_{0.89}\text{CoO}_2$  cobaltite, exhibited a hexagonal structure corresponding to the  $\gamma\text{-Na}_x\text{CoO}_2$  phase structure [11,29,58–60] (Figure 1a). Note that samples of sodium-poor  $\text{Na}_{0.55}\text{Co}_{0.90}\text{Me}_{0.10}\text{O}_2$  cobaltites with the same thermal prehistory [16] contained  $\text{Co}_3\text{O}_4$  impurities formed by the partial degradation of these phases in air. Our results indicate that increasing the sodium content in  $\text{Na}_x\text{CoO}_2$  enhances its chemical stability in air. This conclusion is confirmed by the results of long-term exposure of the samples to wet air, according to which the sodium-rich  $\text{Na}_{0.89}\text{CoO}_2$  compound degrades according to Equations (14) and (15) two times slower than the sodium-poor  $\text{Na}_{0.55}\text{CoO}_2$  phase. The degradation degree of  $\text{Na}_x\text{Co}_{0.90}\text{Me}_{0.10}\text{O}_2$  cobaltites doped with transition or heavy metal oxides, calculated through their mass change, was 7–27% lower than that of the parent  $\text{Na}_x\text{CoO}_2$  phases.

The values of the lattice constants for the  $\text{Na}_{0.89}\text{Co}_{0.90}\text{Me}_{0.10}\text{O}_2$  solid solutions varied within the ranges of  $a = 2.822\text{--}2.831$  Å and  $c = 10.92\text{--}10.97$  Å (Table 1), which are close to the parameters of the  $\text{Na}_{0.89}\text{CoO}_2$  base cobaltite ( $a = 2.826$  Å,  $c = 10.94$  Å) [26,61,62]. As a result, the values of volume of the unit cell for the phases of  $\text{Na}_{0.89}\text{Co}_{0.90}\text{Me}_{0.10}\text{O}_2$  with partial cobalt substitution by transition or heavy metals changed very little, but their axial ratio significantly decreased only with the substitution of cobalt by nickel in the  $\text{Na}_{0.89}\text{CoO}_2$  structure. Thus, partial substitution of cobalt with other metals in the  $\text{Na}_{0.89}\text{CoO}_2$  phase does not lead to significant changes in the size and shape of the unit cell for the  $\text{Na}_{0.89}\text{Co}_{0.90}\text{Me}_{0.10}\text{O}_2$  ( $\text{Me} = \text{Cr, Mo, W, and Bi}$ ) solid solutions compared to the unsubstituted phase of layered sodium cobaltite.

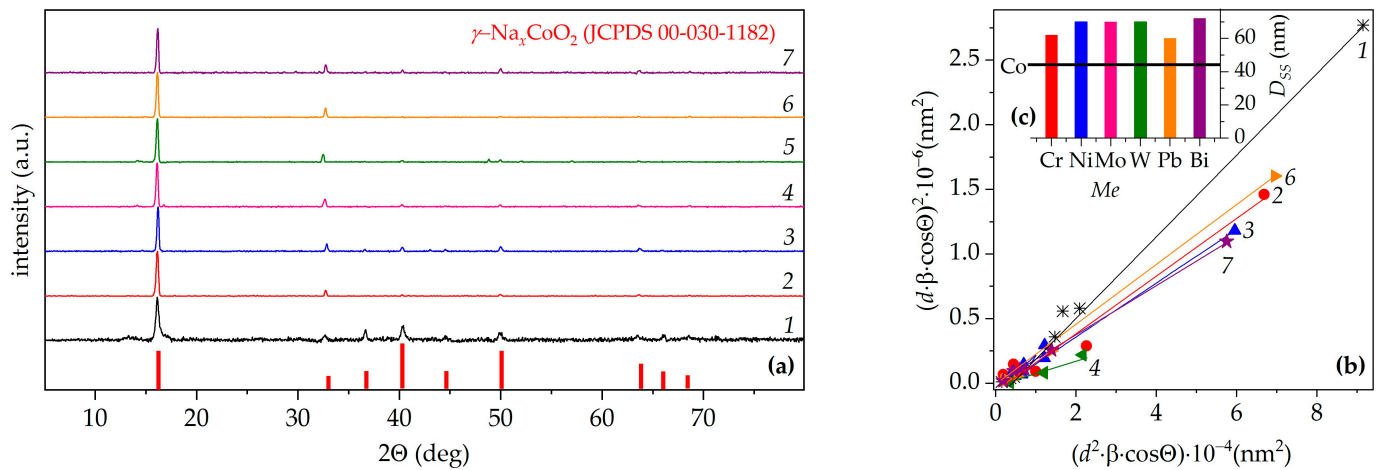


**Figure 1.** X-ray powder diffractograms ( $\text{Cu}_{K\alpha}$ -radiation) (a), size-strain plots (b) and coherent scattering area (c) for  $\text{Na}_{0.89}\text{CoO}_2$  (1, black) layered sodium cobaltite and  $\text{Na}_{0.89}\text{Co}_{0.9}\text{Me}_{0.1}\text{O}_2$  ( $\text{Me} = \text{Cr}$  (2, red), Ni (3, blue), Mo (4, pink), W (5, green), Pb (6, orange), Bi (7, purple)) solid solutions.

The apparent density values of the  $\text{Na}_{0.89}\text{Co}_{0.9}\text{Me}_{0.1}\text{O}_2$  ceramic ranged within 3.18–3.47  $\text{g}/\text{cm}^3$  and decreased with the partial substitution of Co with Cr, Mo, W, or Pb, while they increased with the substitution of Co with Ni and Bi (Table 2). The values of open porosity of the ceramics varied within 16–22% and were close for samples with different cationic compositions, but values of closed porosity were minimal for the base  $\text{Na}_{0.89}\text{CoO}_2$  phase (13%) and  $\text{Na}_{0.89}\text{Co}_{0.9}\text{Ni}_{0.1}\text{O}_2$  solid solution (7%) and for other samples varied within 17–24% and were close each other (Table 2). The values of the apparent density of Na-rich samples were 7–8% less than for Na-poor ones [16], which was probably due to the fact that during heat treatment of ceramics, part of  $\text{Na}_2\text{O}$  evaporates into the environment, and this process intensifies with the increase in sodium content in the samples. In fact, porosity values of the Na-rich samples were about two times larger (Table 2) than for Na-poor ones [16].

**Table 2.** Values of apparent ( $d_{EXP}$ ) density, total ( $\Pi_t$ ), open ( $\Pi_o$ ) and closed ( $\Pi_c$ ) porosity, linear thermal expansion coefficient ( $\alpha$ ), electrical resistivity ( $\rho_{1073}$ ), Seebeck coefficient ( $S_{1073}$ ), power factor ( $P_{1073}$ ) and figure-of-merit ( $ZT_{1073}$ ) of  $\text{Na}_{0.89}\text{Co}_{0.9}\text{Me}_{0.1}\text{O}_2$  ( $\text{Me} = \text{Cr}, \text{Co}, \text{Ni}, \text{Mo}, \text{W}, \text{Pb}, \text{Bi}$ ) ceramics.

$M$	$d_{EXP}, \text{g}/\text{cm}^3$	$\Pi_t, \%$	$\Pi_o, \%$	$\Pi_c, \%$	$10^5 \times \alpha, \text{K}^{-1}$	$10^4 \times \rho_{1073}, \Omega \cdot \text{m}$	$S_{1073}, \mu\text{V}/\text{K}$	$P_{1073}, \text{mW}/(\text{m} \cdot \text{K}^2)$	$\lambda_{1073}, \text{W}/(\text{m} \cdot \text{K})$	$ZT_{1073}$
Cr	3.18	35	16	19	1.68	3.28	134	0.055	0.613	0.10
Co	3.38	32	19	13	1.34	2.43	439	0.794	0.536	1.59
Ni	3.46	29	22	7	1.42	1.50	369	0.910	0.591	1.65
Mo	3.22	36	19	17	1.47	5.73	408	0.291	0.323	0.97
W	3.20	41	17	24	1.39	10.9	519	0.320	0.316	1.09
Pb	3.34	40	18	22	1.26	5.58	358	0.230	0.295	0.84
Bi	3.47	38	18	20	1.25	5.97	616	0.636	0.392	1.74

The Lotgering factor values increased from 0.31 for the  $\text{Na}_{0.89}\text{CoO}_2$  base cobaltite (moderate orientation) to 0.69–0.76 for the  $\text{Na}_{0.89}\text{Co}_{0.9}\text{Me}_{0.1}\text{O}_2$  solid solutions ( $\text{Me} = \text{Ni}$  and Bi) (good orientation) and 0.87–0.92 for the  $\text{Na}_{0.89}\text{Co}_{0.9}\text{Me}_{0.1}\text{O}_2$  ( $\text{Me} = \text{Cr}, \text{Mo}, \text{W}$ , and Pb) ceramics of composition (very good orientation) (Table 1). Thus, doping  $\text{Na}_{0.89}\text{CoO}_2$  with various transition or heavy metal oxides increases the degree of crystallographic orientation of the ceramic grains (the degree of its texturing). The most pronounced effect among the samples synthesized in this work was observed for  $\text{Na}_{0.89}\text{Co}_{0.9}\text{W}_{0.1}\text{O}_2$ , with

the partial substitution of cobalt by tungsten in the  $\text{Na}_{0.55}\text{CoO}_2$  phase leading to a similar effect [16,48].

The coherent scattering area of the  $\text{Na}_{0.89}\text{Co}_{0.90}\text{Me}_{0.10}\text{O}_2$  materials, synthesized in this study, calculated using different approaches (Figure 1b), was larger (up to 6–25% and 3360% according to the Debye–Scherrer and the size-strain method, respectively) comparing to the base layered sodium cobaltite phase (Figure 1b, Table 1). In turn, the values of microstrains for the  $\text{Na}_{0.89}\text{Co}_{0.90}\text{Me}_{0.10}\text{O}_2$  ceramics were slightly ( $\text{Me} = \text{Cr}$  and  $\text{Pb}$ ) or significantly ( $\text{Me} = \text{Ni}$ ,  $\text{Mo}$ ,  $\text{W}$ , and  $\text{Bi}$ ) lower compared to the initial  $\text{Na}_{0.89}\text{CoO}_2$  cobaltite (Table 1). Therefore, the partial substitution of cobalt by transition or heavy metals in  $\text{Na}_{0.89}\text{CoO}_2$  results in the formation of ceramics with larger-grained and less-strained grains.

According to the results of SEM, the grains of the  $\text{Na}_{0.89}\text{CoO}_2$  base unsubstituted cobaltite had a plate-like shape with dimensions ( $l$ ) of 6–15  $\mu\text{m}$  and a thickness of 2.5–3  $\mu\text{m}$  (with an average size ( $l_{av}$ ) of about 7  $\mu\text{m}$  and an aspect ratio ( $AR$ ) of approximately 3.9) (Figure 2b). The microstructure of the  $\text{Na}_{0.89}\text{Co}_{0.90}\text{M}_{0.10}\text{O}_2$  materials was similar to that of  $\text{Na}_{0.89}\text{CoO}_2$ , but it differed in the size and aspect ratio (shape) of the grains (Figure 2a,c–f).

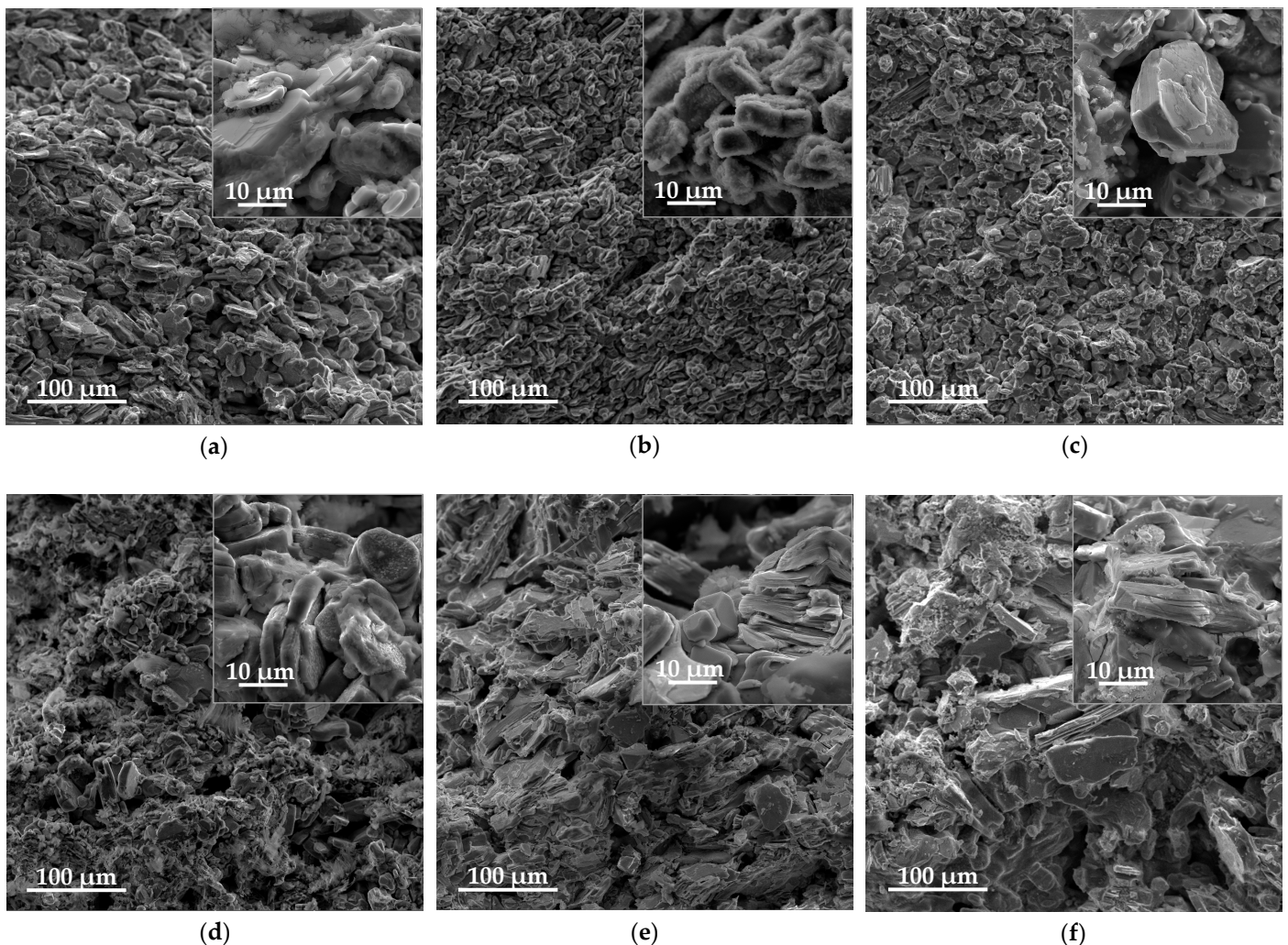


**Figure 2.** Electronic micrographs of ceramic cleavage of  $\text{Na}_{0.89}\text{Co}_{0.9}\text{M}_{0.1}\text{O}_2$  ( $\text{M} = \text{Cr}$  (a),  $\text{Co}$  (b),  $\text{Ni}$  (c),  $\text{W}$  (d),  $\text{Pb}$  (e),  $\text{Bi}$  (f)).

The grain sizes of the  $\text{Na}_{0.89}\text{Co}_{0.90}\text{Me}_{0.10}\text{O}_2$  ( $\text{Me} = \text{Cr}$ ,  $\text{Ni}$ ,  $\text{W}$ ) ceramics varied within 6–23  $\mu\text{m}$ , with a thickness of 6–10  $\mu\text{m}$ . The average dimensions ( $l_{av}$  ( $AR$ )) were approximately 17  $\mu\text{m}$  (2.8) for  $\text{Me} = \text{Cr}$ , 22  $\mu\text{m}$  (3.3) for  $\text{Me} = \text{Ni}$ , and 14  $\mu\text{m}$  (3.2) for  $\text{Me} = \text{W}$ . Doping of the layered sodium cobaltite ceramics with bismuth or lead oxides resulted in an increase

in grain size to 35–60  $\mu\text{m}$  and a decrease in the thickness of the grains by up to 1–3  $\mu\text{m}$ . For  $\text{Na}_{0.89}\text{Co}_{0.90}\text{Pb}_{0.10}\text{O}_2$  and  $\text{Na}_{0.89}\text{Co}_{0.90}\text{Bi}_{0.10}\text{O}_2$ , the  $l_{av}$  ( $AR$ ) values were around 43  $\mu\text{m}$  (14.3) and 52  $\mu\text{m}$  (15.6), respectively. Consequently, the anisotropy of the grains in the sodium cobaltite ceramic increased with doping by heavy metal oxides ( $\text{PbO}$  and  $\text{Bi}_2\text{O}_3$ ).

The enhancement of the Lotgering factor and improvement of the anisotropy degree ( $AR$ ) of the grains of  $\text{Na}_{0.89}\text{Co}_{0.90}\text{Me}_{0.10}\text{O}_2$  ceramics may be caused by the differences in the sizes of the substituting and substituted ions (size effect) and their charges (charge redistribution). The first results in localized lattice strain promoting preferential alignment of grains along specific crystallographic planes (in our case,  $(00l)$ ), but the second alters the charge distribution in the structure of  $\text{Na}_{0.89}\text{Co}_{0.90}\text{Me}_{0.10}\text{O}_2$  phases, enhances interlayer charge screening, reduces electrostatic repulsion of  $\text{CoO}_2$ -layers, and stabilizes  $(00l)$ -oriented stacking. The maximal values of  $f$  and  $AR$  were observed, in the whole, for the samples of layered sodium cobaltite, doped by heavy metal oxides ( $\text{Pb}$ ,  $\text{W}$  etc.) (Table 1, Figure 2), as in these cases, the maximal difference in the sizes and charges of the substituting and substituted ions occurs.

According to the EDX results, the cationic composition of the  $\text{Na}_{0.89}\text{Co}_{0.90}\text{M}_{0.10}\text{O}_2$  synthesized compounds was close to the target values, and the distribution of elements within the ceramic was nearly uniform (Figures 3 and S2 (see Supplementary Information)).

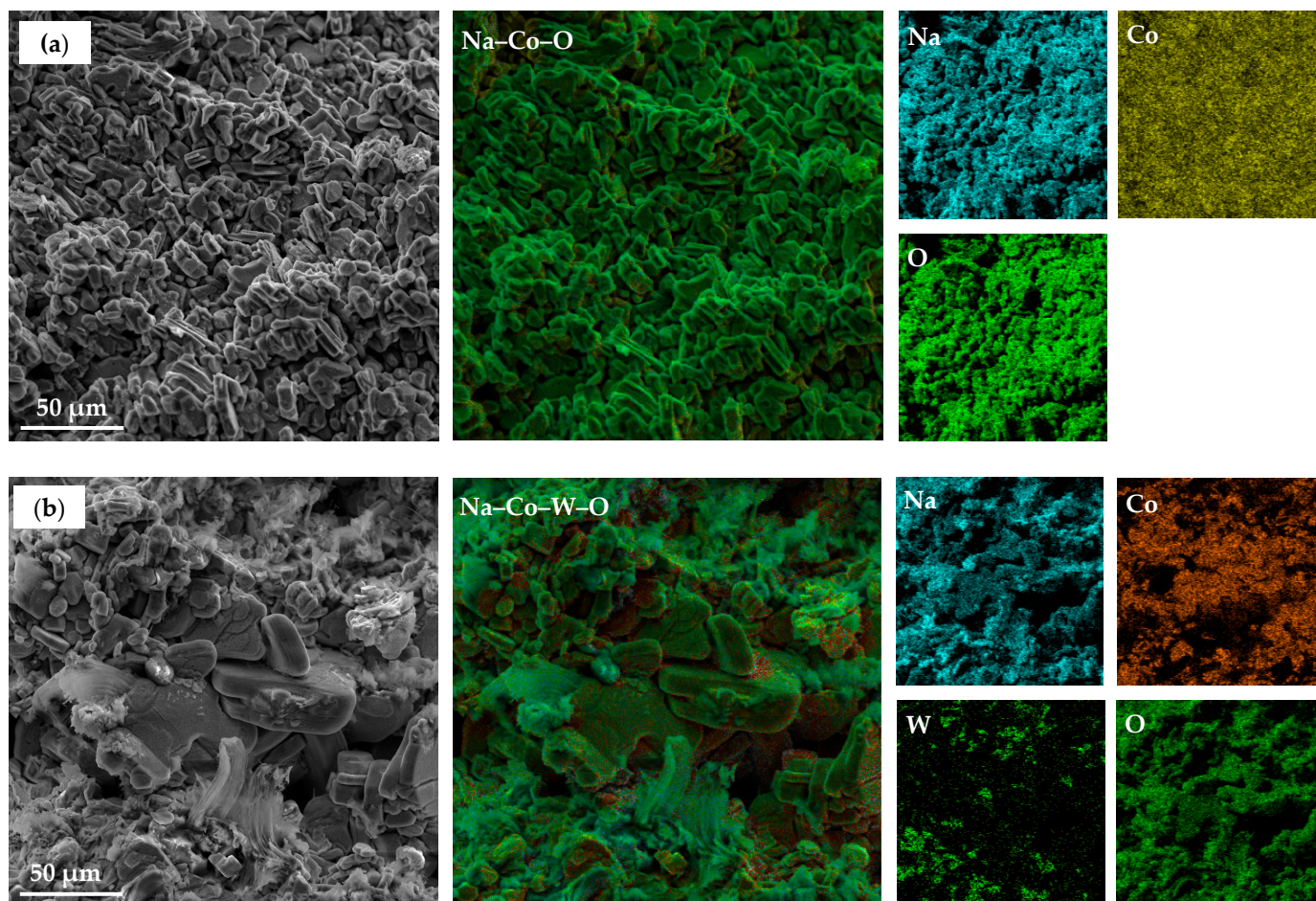


**Figure 3.** Element mapping images of the  $\text{Na}_{0.89}\text{Co}_{0.90}\text{O}_2$  (a) and  $\text{Na}_{0.89}\text{Co}_{0.9}\text{W}_{0.1}\text{O}_2$  (b) ceramic samples.

The Temperature dependence of the relative elongation of the  $\text{Na}_{0.89}\text{Co}_{0.9}\text{Me}_{0.1}\text{O}_2$  ceramic samples was practically linear, which proves the absence of structural phase transitions in the complex oxides investigated within all the temperature intervals studied. LTEC values of the  $\text{Na}_{0.89}\text{Co}_{0.9}\text{Me}_{0.1}\text{O}_2$  solid solutions varied within  $(1.25\text{--}1.68) \times 10^{-5} \text{ K}^{-1}$  and

were lower (for  $Me = Pb$ , and  $Bi$ ), slightly (for  $Me = W$ ) and essentially larger (for  $Me = Cr$ ,  $Ni$ , and  $Mo$ ) than for unsubstituted sodium cobaltite  $Na_{0.89}CoO_2$  ( $1.34 \times 10^{-5} K^{-5}$ ) (Table 2).

The increase in the LTEC values of the  $Na_{0.89}Co_{0.90}Me_{0.10}O_2$  derivatives compared to those of the  $Na_{0.89}CoO_2$  base phase is possibly due to the high values of their porosity (Table 2) as well as to the increase in the anharmonicity of the metal–oxygen vibrations in their structure with partial substitution of cobalt by other metals.

As can be seen from the Figure 4a, the  $Na_{0.89}CoO_2$  layered sodium cobaltite and its  $Na_{0.89}Co_{0.90}Me_{0.10}O_2$  derivatives exhibited metallic-like conductivity character ( $\partial\rho/\partial T > 0$ ) (except  $Na_{0.89}Co_{0.90}W_{0.10}O_2$  solid solution, which possesses semiconducting conductivity character within all the temperature interval studied), which for the  $Na_{0.89}Co_{0.90}Bi_{0.10}O_2$  and  $Na_{0.89}Co_{0.90}Mo_{0.10}O_2$  solid solutions near 923 K changed into a semiconducting one ( $\partial\rho/\partial T < 0$ ) like the conductivity crossover in layered calcium cobaltite of  $Ca_3Co_4O_{9+\delta}$  [63,64]. A similar effect was also observed in several  $Na_{0.55}Co_{0.90}Me_{0.10}O_2$  layered sodium cobaltites earlier [16]. The doping of  $Na_{0.89}CoO_2$  layered sodium cobaltite by different metal oxides results in increasing its electrical resistivity values, except  $NiO$ , as  $\rho$  values of  $Na_{0.89}Co_{0.90}Ni_{0.10}O_2$  solid solution were essentially less than those for the unsubstituted layered sodium cobaltite (Figure 4a,d). The metallic-like conductivity and low  $\rho$  values of the  $Ni$ -doped layered cobaltite are in good agreement with the results of [40,41] and are due to the donor nature of the substitution of  $Co$  by  $Ni$ , resulting in an increase in the concentration of holes, which are the main charge carriers in the layered sodium cobaltites. As can be seen, electrical resistivity values of ceramics increased with the increase in oxidation state of the substituting cobalt metal  $Me$  ( $\rho(Na_{0.89}Co_{0.90}Ni_{0.10}O_2) < \rho(Na_{0.89}CoO_2) < \rho(Na_{0.89}Co_{0.90}Pb_{0.10}O_2)$ ). This can be explained by a decrease in the concentration of the main charge carriers (holes) as the average oxidation state of the cations in the conducting  $(Co,Me)O_2$  layers of the crystal structure  $Na_{0.89}Co_{0.90}Me_{0.10}O_2$  phases increased (Figure 4a,d, Table 2).

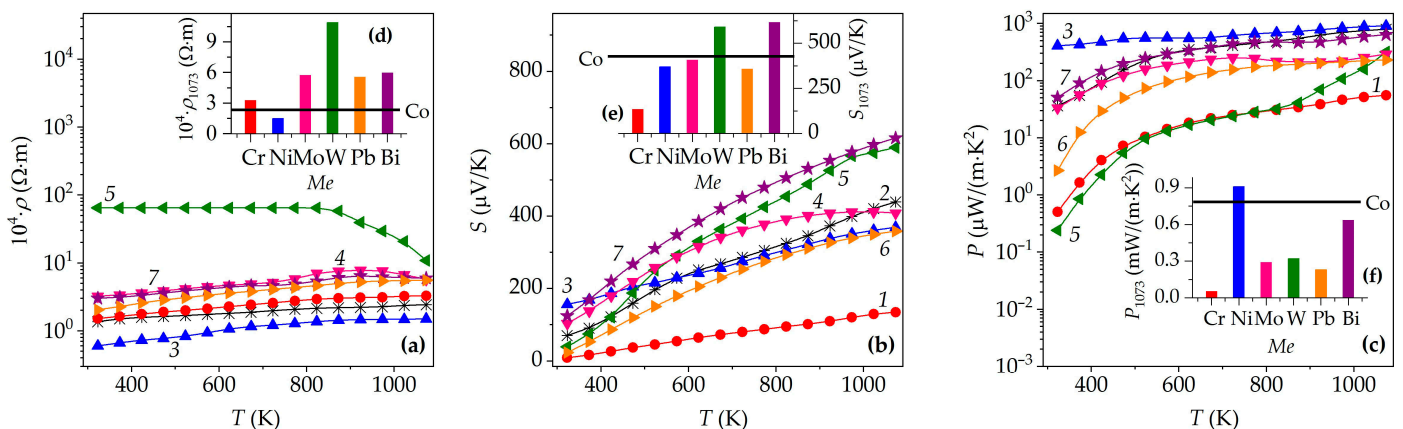


**Figure 4.** Temperature dependences of electrical resistivity  $\rho$  (a), Seebeck's coefficient  $S$  (b) and power factor  $P$  (c) of ceramic samples of  $Na_{0.89}Co_{0.9}Me_{0.1}O_2$  ( $Me = Cr$  (1, red),  $Co$  (2, black),  $Ni$  (3, blue),  $Mo$  (4, pink),  $W$  (5, green),  $Pb$  (6, orange),  $Bi$  (7, purple)). Insets show the electrical resistivity  $\rho_{1073}$  (d), Seebeck's coefficient  $S_{1073}$  (e), and power factor  $P_{1073}$  (f) values of  $Na_{0.89}Co_{0.9}Me_{0.1}O_2$  phases.

The electrical resistivity of oxide ceramics is affected by their chemical and phase compositions, as well as their microstructural characteristics, such as porosity. In our case, namely larger  $\Pi_t$  values explain the facts, that  $\rho(Na_{0.89}Co_{0.90}Cr_{0.10}O_2) > \rho(Na_{0.89}CoO_2)$ ,  $\rho(Na_{0.89}Co_{0.90}W_{0.10}O_2) > \rho(Na_{0.89}Co_{0.90}Mo_{0.10}O_2)$  (Figure 4a,d, Table 2) though according average oxidation state of cobalt (Table 1) these pairs of  $Na_{0.89}Co_{0.90}Me_{0.10}O_2$  ceramic samples should demonstrate close values of electrical resistivity.

The electrical resistivity values of the  $\text{Na}_{0.89}\text{Co}_{0.90}\text{Me}_{0.10}\text{O}_2$  ceramic samples did not change after several thermocycles, exposure to wet air for two weeks, and annealing in air at 1073 K for eight hours. Note that the  $\rho$  values of  $\text{Na}_{0.55}\text{Co}_{0.90}\text{Me}_{0.10}\text{O}_2$  compounds [16] aged under the same schemes increased by 15–25% depending on their composition. These facts prove the enhancement of the chemical and thermal stability of layered sodium cobaltite and its derivatives with increasing sodium content, and allow us to consider the sodium-rich  $\text{Na}_{0.89}\text{Co}_{0.90}\text{Me}_{0.10}\text{O}_2$  compounds as more suitable for different practical purposes than sodium-poor ones.

The Seebeck coefficient of the  $\text{Na}_{0.89}\text{Co}_{0.90}\text{Me}_{0.10}\text{O}_2$  ( $\text{Me} = \text{Cr, Ni, Mo, W, Pb, and Bi}$ ) solid solutions was positive throughout the temperature range studied, indicating that the main charge carriers were holes, and these materials were classified as  $p$ -type conductors. Notably, at high temperatures, the change in the thermo-EMF for all materials studied was nearly linear. This relationship of the Seebeck coefficient corresponds to Equation (16), which is commonly used to describe the thermoelectric properties of metals and degenerate semiconductors [65]

$$S = \left( \frac{8 \cdot \pi^2 \cdot k_B^2}{3 \cdot e \cdot h} \right) \cdot m^* \cdot T \cdot \left( \frac{\pi}{3 \cdot n} \right)^{2/3}, \quad (16)$$

where  $k_B$  is the Boltzmann constant (J/K),  $m^*$  is the density of the effective mass (kg),  $h$  is the Planck's constant (J·s),  $e$  is the charge of the electron (C),  $T$  is the absolute temperature (K), and  $n$  is the charge carrier concentration ( $\text{cm}^{-3}$ ).

The partial substitution of cobalt with ions of various transition or heavy metals in the structure of  $\text{Na}_{0.89}\text{CoO}_2$  led to an increase in the Seebeck coefficient, which was more pronounced at high temperatures for tungsten- or bismuth-substituted solid solutions (Figure 4b,e, and Table 2). This is likely due to the increase in configurational entropy provided by the presence of cobalt ions with different charges ( $\text{Co}^{2+}$ ,  $\text{Co}^{3+}$ , and  $\text{Co}^{4+}$ ) and spin states (high, intermediate, and low spin). The fact that the Seebeck coefficient values of the  $\text{Na}_{0.89}\text{Co}_{0.90}\text{W}_{0.10}\text{O}_2$  phase are larger than those of the  $\text{Na}_{0.89}\text{Co}_{0.90}\text{Mo}_{0.10}\text{O}_2$  cobaltite, in which cobalt possesses the same oxidation state and spin state, may be due to its larger porosity. The highest values of  $S$  among all investigated samples were demonstrated by the  $\text{Na}_{0.89}\text{Co}_{0.90}\text{W}_{0.10}\text{O}_2$  and  $\text{Na}_{0.89}\text{Co}_{0.90}\text{Bi}_{0.10}\text{O}_2$  oxides (519 and 616  $\mu\text{V/K}$  at 1073 K, respectively), which are 1.18 and 1.40 times larger than that of the parent  $\text{Na}_{0.89}\text{CoO}_2$  phase (Figure 4e and Table 2). Therefore, these phases can be considered as prospective materials for the  $p$ -legs of ceramic (oxide) thermocouples. It should also be noted that similar results were obtained when studying the Seebeck coefficient of cobalt-substituted derivatives of the  $\text{Na}_{0.55}\text{CoO}_2$  layered cobaltite [16,38]. The Seebeck coefficient of the  $\text{Na}_{0.89}\text{Co}_{0.90}\text{Me}_{0.10}\text{O}_2$  phases after exposure to wet air for two weeks remained the same within the accuracy of the measurements. In contrast, aged under the same conditions,  $\text{Na}_{0.55}\text{Co}_{0.90}\text{Me}_{0.10}\text{O}_2$  samples demonstrated an increase in their  $S$  value up to 15–25% depending on their composition, which looks like the results of  $\rho$  measurements proved their lower chemical stability.

The weighted mobility ( $\mu_p$ ) and concentration ( $p$ ) of the main charge carriers («holes») in the samples studied, calculated based on the experimentally determined  $\rho$  and  $S$  values according to the method described in [66] (see Supplementary Information, Equations (S8) and (S9)), varied with temperature change and essentially and non-monotonously changed when  $\text{Na}_{0.89}\text{CoO}_2$  was doped with different metal oxides. For the base  $\text{Na}_{0.89}\text{CoO}_2$  cobaltite at 1073 K, the values of  $\mu_p$  and  $p$  were  $\sim 48 \text{ cm}^2/(\text{V}\cdot\text{s})$  and  $\sim 5 \times 10^{-20} \text{ cm}^{-3}$ , respectively, which is in good agreement with the literature data [67]. The weighted mobility values of the  $\text{Na}_{0.89}\text{Co}_{0.90}\text{Me}_{0.10}\text{O}_2$  solid solutions were less than, close to, and larger than those of  $\text{Na}_{0.89}\text{CoO}_2$  for  $\text{Me} = \text{Cr, Mo, Pb, Me} = \text{Ni, W, and Me} = \text{Bi}$ , respectively. Charge carriers concentration in  $\text{Na}_{0.89}\text{Co}_{0.90}\text{Me}_{0.10}\text{O}_2$  cobaltites was large, close to, and less, than for  $\text{Na}_{0.89}\text{CoO}_2$  phase for  $\text{Me} = \text{Cr, Me} = \text{Mo, Ni, Pb, and Me} = \text{W}$ ,

Bi respectively, that is in good accordance with the results of measurements of Seebeck coefficient of ceramics, for example, with the sharp increasing of  $S$  values of the layered sodium cobaltite at partial substitution of cobalt by bismuth or tungsten in it, and with the sharp decreasing of  $S$  at partial substitution of cobalt by chromium in  $\text{Na}_{0.89}\text{CoO}_2$  (Figure 4b,e).

The power factor values of  $\text{Na}_{0.89}\text{Co}_{0.90}\text{Me}_{0.10}\text{O}_2$  sintered ceramics increased with rising temperature and changed non-monotonically with the changing of the nature of metal substituting cobalt in the  $\text{Na}_{0.89}\text{CoO}_2$  structure (Figure 4c,f, and Table 2). The maximum  $p$  value was achieved for the  $\text{Na}_{0.89}\text{Co}_{0.90}\text{Ni}_{0.10}\text{O}_2$  nickel-substituted solid solution ( $0.910 \text{ mW}/(\text{m}\cdot\text{K}^2)$ ) at 1073 K, which is 1.15 times larger than that of the undoped  $\text{Na}_{0.89}\text{CoO}_2$  layered sodium cobaltite, and was determined by both the low values of its electrical resistivity and high values of its Seebeck's coefficient.

The thermal diffusivity and thermal conductivity values of the  $\text{Na}_{0.89}\text{Co}_{0.10}\text{Me}_{0.10}\text{O}_2$  ceramics decreased with increasing of temperature (Figure 5a,b) and changed non-monotonously at the doping of  $\text{Na}_{0.89}\text{CoO}_2$  by various metal oxides, increasing at substitution of Co by Cr, and Ni, and decreasing at substitution of Co by Mo, W, Pb, and Bi (Figure 5d,e). The first is associated with an increase in the grain size of the ceramics, which leads to a decrease in the density of grain boundaries that serve as effective phonon scattering regions. The latter occurs due to the partial replacement of lighter cobalt ions by heavier ions of molybdenum, tungsten, lead, or bismuth, serving as effective scattering centers. The electronic component of the thermal conductivity of the ceramics was relatively small ( $\lambda_e/\lambda = 0.03\text{--}0.13$ ) and increased with increasing temperature, and for the  $\text{Na}_{0.89}\text{Co}_{0.10}\text{Me}_{0.10}\text{O}_2$  solid solutions, except  $\text{Na}_{0.89}\text{Co}_{0.90}\text{Ni}_{0.10}\text{O}_2$ , it was lower than that of the  $\text{Na}_{0.89}\text{CoO}_2$  base oxide. Thus, the main part of the heat in the  $\text{Na}_{0.89}\text{Co}_{0.10}\text{Me}_{0.10}\text{O}_2$  phases was carried by lattice vibrations (phonons) ( $\lambda_{ph}/\lambda \approx (0.87\text{--}0.97)$ ) (Figure 5c,f). As shown in Figure 5, the thermal diffusivity and conductivity values of the doped cobaltites (except Cr- and Ni-doped) are lower than those of the base  $\text{Na}_{0.89}\text{CoO}_2$  phase. It should be noted that for sodium-poor samples ( $\text{Na}_{0.55}\text{Co}_{0.90}\text{Me}_{0.10}\text{O}_2$ ), the converse effect was found, namely an increase in  $\eta$  and  $\lambda$  values of doped with transition or heavy metal oxides ceramics compared to the undoped  $\text{Na}_{0.55}\text{CoO}_2$  phase [16,38].

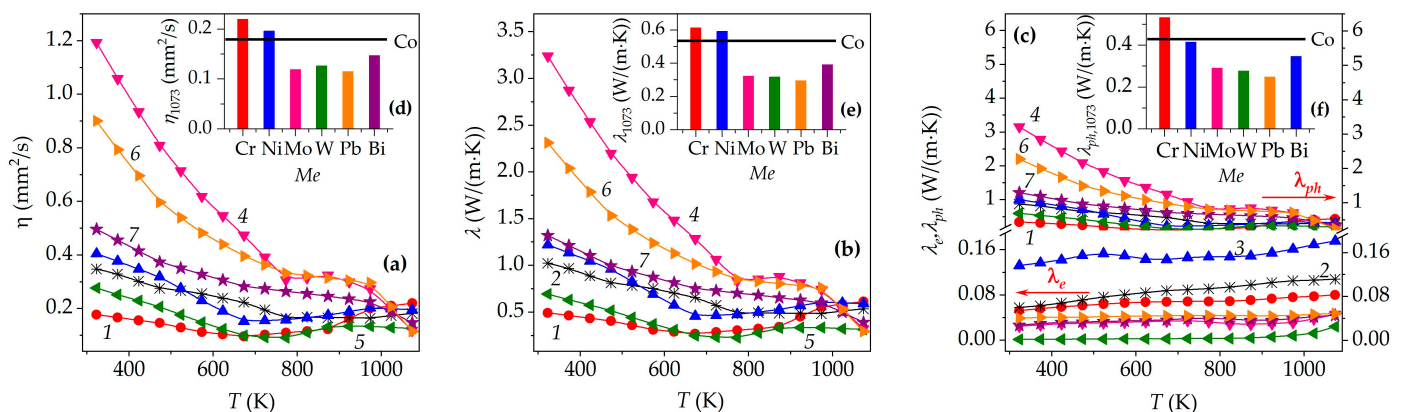


**Figure 5.** Temperature dependences of thermal diffusivity  $\eta$  (a), total thermal conductivity  $\lambda$  (b), phonon  $\lambda_{ph}$  and electron  $\lambda_e$  contributions (c) in thermal conductivity of  $\text{Na}_{0.89}\text{Co}_{0.9}\text{Me}_{0.1}\text{O}_2$  ( $\text{Me} = \text{Cr}$  (1, red), Co (2, black), Ni (3, blue), Mo (4, pink), W (5, green), Pb (6, orange), Bi (7, purple)) ceramic samples. Insets show the thermal diffusivity  $\eta_{1073}$  (d), total thermal conductivity  $\lambda_{1073}$  (e) and phonon thermal conductivity  $\lambda_{ph,1073}$  (f) of  $\text{Na}_{0.89}\text{Co}_{0.9}\text{Me}_{0.1}\text{O}_2$  materials.

Although the porosity values of the  $\text{Na}_{0.89}\text{Co}_{0.90}\text{Me}_{0.10}\text{O}_2$  ceramic samples were similar (Table 2), some effects of  $\Pi_t$  on the thermal properties of the layered sodium cobaltite derivatives were observed and should be noted. Therefore, the fact that the  $\text{Na}_{0.89}\text{Co}_{0.90}\text{Bi}_{0.10}\text{O}_2$

sample demonstrates larger  $\eta$ ,  $\lambda$ , and  $\lambda_{ph}$  values than the  $\text{Na}_{0.89}\text{Co}_{0.90}\text{Pb}_{0.10}\text{O}_2$  solid solution (Figure 5) is probably due to its lower porosity.

The figure of merit values of the investigated materials sharply increased with increasing temperature, and doping of layered sodium cobaltite with various transition and heavy metal oxides had different effects:  $ZT$  increased at substitution in  $\text{Na}_{0.89}\text{CoO}_2$  of cobalt by nickel and bismuth and decreased when cobalt was partially substituted by chromium, molybdenum, tungsten, and lead (Figure 6a and Table 2). The highest thermoelectric characteristics were demonstrated by  $\text{Na}_{0.89}\text{Co}_{0.90}\text{Ni}_{0.10}\text{O}_2$  and  $\text{Na}_{0.89}\text{Co}_{0.90}\text{Bi}_{0.10}\text{O}_2$  solid solutions, with  $ZT$  values reaching 1.65 and 1.74 at 1073 K, which are about 4% and 9% higher, respectively, than that of the  $\text{Na}_{0.89}\text{CoO}_2$  phase (Figure 6c). It should be noted that although for the  $\text{Na}_{0.89}\text{Co}_{0.90}\text{W}_{0.10}\text{O}_2$ ,  $\text{Na}_{0.89}\text{Co}_{0.90}\text{Mo}_{0.10}\text{O}_2$ , and  $\text{Na}_{0.89}\text{Co}_{0.90}\text{Pb}_{0.10}\text{O}_2$  ceramics  $ZT$  values were less than that of the  $\text{Na}_{0.89}\text{CoO}_2$  phase, at 1073 K, they were equal to 1.09, 0.97, and 0.84, respectively, which is close to the theoretical criterion ( $ZT > 1$ ) that defines materials of practical interest for thermoelectric conversion (Figure 6a and Table 2).

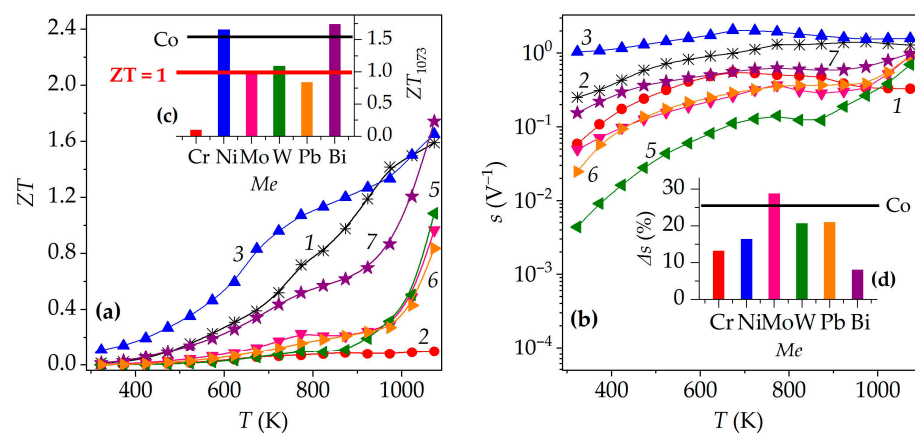


**Figure 6.** Temperature dependences of figure-of-merit  $ZT$  (a) and self-compatibility factor  $s$  (b) of  $\text{Na}_{0.89}\text{Co}_{0.9}\text{Me}_{0.1}\text{O}_2$  ( $\text{Me} = \text{Cr}$  (1, red), Co (2, black), Ni (3, blue), Mo (4, pink), W (5, green), Pb (6, orange), Bi (7, purple)) ceramic samples. Insets show the figure-of-merit  $ZT_{1073}$  (c) and dimensionless relative self-compatibility factor  $\Delta s_{673-873\text{K}}$  (d) (within 673–873 K temperature range) of  $\text{Na}_{0.89}\text{Co}_{0.90}\text{Me}_{0.10}\text{O}_2$  ceramics.

The self-compatibility factor values ( $s$ ) of the ceramics studied increased at temperature increasing and within temperature interval 673–873 K slightly vary (except for  $\text{Na}_{0.89}\text{Co}_{0.90}\text{Cr}_{0.10}\text{O}_2$  compound) (Figure 6b), and dimensionless relative self-compatibility factor ( $\Delta s$ ) of  $\text{Na}_{0.89}\text{Co}_{0.90}\text{Me}_{0.10}\text{O}_2$  layered cobaltites within 673–873 K varies within 8–29% (Figure 6d), which is, in the whole, less than for the  $\text{Mg}_2\text{Si}_{0.6-y}\text{Sn}_{0.4}\text{Sb}_y$  (25–40%) thermoelectric alloy [68] and states the good self-compatibility of the obtained in this work thermoelectric oxide ceramics. Note, that  $\Delta s$  values for the doped sodium cobaltites, except  $\text{Na}_{0.89}\text{Co}_{0.90}\text{Mo}_{0.10}\text{O}_2$ , were less (8–21%) than for the base layered sodium cobaltite (26%), which shows the effectiveness of doping of  $\text{Na}_{0.89}\text{CoO}_2$  by transition or heavy metal oxides in increasing of its self-compatibility.

Comparing the results obtained in this study with the data published in [16], we can conclude that the modification of layered sodium cobaltite by different metal oxides similarly affects its structure and properties for both sodium-rich ( $\text{Na}_{0.89}\text{Co}_{0.90}\text{Me}_{0.10}\text{O}_2$ ) and sodium-poor ( $\text{Na}_{0.55}\text{Co}_{0.90}\text{Me}_{0.10}\text{O}_2$ ) samples. However, for the latter, the effect is more pronounced due to the larger  $\rho$  and smaller  $S$  values for the  $\text{Na}_{0.55}\text{CoO}_2$  phase. In contrast, sodium-rich  $\text{Na}_{0.89}\text{Co}_{0.90}\text{Me}_{0.10}\text{O}_2$  compounds demonstrate higher chemical and thermal stabilities than sodium-poor  $\text{Na}_{0.55}\text{Co}_{0.90}\text{Me}_{0.10}\text{O}_2$  phases under both storage and operating conditions. This fact, along with their superior thermoelectric characteristics,

makes  $\text{Na}_{0.89}\text{Co}_{0.90}\text{Me}_{0.10}\text{O}_2$  cobaltites more suitable for practical applications in different thermoelectric devices (ceramic thermocouples, thermoelectric generators, and industrial waste heat recovery systems).

It should also be noted that layered sodium cobaltite and its derivatives demonstrate significantly larger Seebeck coefficients, power factors, and figure-of-merit values than other layered cobaltites ( $\text{Ca}_3\text{Co}_4\text{O}_{9+\delta}$ ,  $\text{Bi}_2\text{Ca}_2\text{Co}_{1.7}\text{O}_y$ , etc.) [6,9,69–71]; therefore, they can be considered more promising thermoelectric materials.

#### 4. Conclusions

Combining the results obtained in this study, one can conclude that doping (up to 10 mol.%) of  $\text{Na}_{0.89}\text{CoO}_2$  sodium-rich layered cobaltite by different transition ( $\text{Cr}_2\text{O}_3$ ,  $\text{NiO}$ ) and heavy metal oxides ( $\text{MoO}_3$ ,  $\text{WO}_3$ ,  $\text{PbO}$ ,  $\text{Bi}_2\text{O}_3$ ) do not change its crystal structure and slightly affects its lattice constants values, but increases coherent scattering area values, grains size as well as grain orientation degree of  $\text{Na}_{0.89}\text{Co}_{0.10}\text{Me}_{0.10}\text{O}_2$  solid solutions comparing to the parent  $\text{Na}_{0.89}\text{CoO}_2$  phase.

Such doping leads to a decrease in the electrical resistivity of the samples and complex changes in the Seebeck coefficient and thermal properties of the ceramics, which are determined by the nature of the metal substituting cobalt in  $\text{Na}_{0.89}\text{CoO}_2$  and the peculiarities of the microstructure of the ceramics. The highest values of  $S$  possessed by the  $\text{Na}_{0.89}\text{Co}_{0.90}\text{W}_{0.10}\text{O}_2$  and  $\text{Na}_{0.89}\text{Co}_{0.90}\text{Bi}_{0.10}\text{O}_2$  cobaltites (519 and 616  $\mu\text{V}/\text{K}$ , respectively, at 1073 K), which are 18% and 40% higher than that of the parent  $\text{Na}_{0.89}\text{CoO}_2$  phase.

The maximal power factor was observed for the  $\text{Na}_{0.89}\text{Co}_{0.90}\text{Ni}_{0.10}\text{O}_2$  compound (0.910  $\text{mW}/(\text{m}\cdot\text{K}^2)$  at 1073 K), which was 15% higher than that of the base  $\text{Na}_{0.89}\text{CoO}_2$  layered sodium cobaltite, which was attributed to both the low values of its electrical resistivity and high values of its Seebeck coefficient. The largest thermoelectric performance was demonstrated by the  $\text{Na}_{0.89}\text{Co}_{0.90}\text{Ni}_{0.10}\text{O}_2$  and  $\text{Na}_{0.89}\text{Co}_{0.90}\text{Bi}_{0.10}\text{O}_2$  phases, with  $ZT$  values of 1.65 and 1.74 at 1073 K, which were about 4% and 9% higher, respectively, than that of the  $\text{Na}_{0.89}\text{CoO}_2$  phase.

The obtained results demonstrate the effectiveness of the doping strategy of cobalt by heavy metals in layered sodium cobaltite for the enhancement of the thermoelectric performance of cobaltite derivatives. It was also found that the dimensionless relative self-compatibility factor of  $\text{Na}_{0.89}\text{CoO}_2$  layered sodium cobaltite is essentially reduced by doping with transition or heavy metal oxides.

The high sodium content ( $\text{Na}:\text{Co}:\text{Me} = 0.89:0.90:0.10$ ) in these phases provides enhanced thermal and chemical stability compared to the phases with low sodium content ( $\text{Na}:\text{Co}:\text{Me} = 0.55:0.90:0.10$ ), which makes the former more promising candidates for thermoelectric devices. Materials possessing high Seebeck coefficient values ( $\text{Na}_{0.89}\text{Co}_{0.90}\text{Me}_{0.10}\text{O}_2$  ( $\text{Me} = \text{W}, \text{Bi}$ )) are suitable for use in thermocouples, but compounds with large values of power factors and figure-of-merit ( $\text{Na}_{0.89}\text{Co}_{0.90}\text{Me}_{0.10}\text{O}_2$  ( $\text{Me} = \text{Ni}, \text{Bi}$ )) can be used as components of thermoelectric generators and industrial waste heat recovery systems.

**Supplementary Materials:** The following supporting information can be downloaded at: <https://www.mdpi.com/article/10.3390/ceramics8030086/s1>. Figure S1: Absorption spectra and calibration graphs for determining the cobalt content in the form of complexes  $[\text{Co}(\text{SCN})_4]^{2-}$  (a, c) и  $[\text{CoY}]^-$  (b, d); Figure S2: Element mapping images of the  $\text{Na}_{0.89}\text{Co}_{0.90}\text{M}_{0.10}\text{O}_2$  ceramic samples ( $\text{M} = \text{Cr}$  (a),  $\text{Ni}$  (b),  $\text{Pb}$  (c),  $\text{Bi}$  (d)); Table S1: Sodium content ( $x_{\text{Na}}$ ) and average oxidation state of cobalt ( $Z$ ) in  $\text{Na}_{0.89}\text{Co}_{0.90}\text{M}_{0.10}\text{O}_2$  layered cobaltite samples determined by various methods.

**Author Contributions:** Conceptualization, A.I.K.; methodology, A.I.K., E.A.C. and N.S.K.; software, N.S.K.; validation, A.I.K., E.A.C. and H.W.; formal analysis, N.S.K. and E.A.C.; investigation, N.S.K., J.A.Z. and A.V.B.; resources, A.I.K.; data curation, A.I.K.; writing—original draft preparation, N.S.K.

and A.I.K.; writing—review and editing, A.I.K. and H.W.; visualization, N.S.K.; supervision, A.I.K.; project administration, A.I.K.; funding acquisition, A.I.K. and N.S.K. All authors have read and agreed to the published version of the manuscript.

**Funding:** This work was supported by the Ministry of Education of the Republic of Belarus under project number 20111575 and by the Belarusian Republican Foundation for Fundamental Research under project number 20122443.

**Institutional Review Board Statement:** Not applicable.

**Informed Consent Statement:** Not applicable.

**Data Availability Statement:** All data generated or analyzed during this study are included in this published article.

**Acknowledgments:** The authors would like to thank Dzmitry S. Kharytonau for fruitful discussions on the research results and Dzmitry Darashchuk for technical support.

**Conflicts of Interest:** The authors declare no conflicts of interest.

## References

1. Klyndyuk, A.I.; Kharytonau, D.S.; Matsukevich, I.V.; Chizhova, E.A.; Lenčėš, Z.; Socha, R.P.; Zimowska, M.; Hanzel, O.; Janek, M. Effect of cationic nonstoichiometry on thermoelectric properties of layered calcium cobaltite obtained by field assisted sintering technology (FAST). *Ceram. Int.* **2024**, *50*, 30970–30979. [[CrossRef](#)]
2. Polevik, A.O.; Sobolev, A.V.; Glazcova, I.S.; Presniakov, I.A.; Verchenko, V.Y.; Link, J.; Stern, R.; Shevelkov, A.V. Interplay between Fe(II) and Fe(III) and Its Impact on Thermoelectric Properties of Iron-Substituted Colusites  $\text{Cu}_{26-x}\text{Fe}_x\text{V}_2\text{Sn}_6\text{S}_{32}$ . *Compounds* **2023**, *3*, 348–364. [[CrossRef](#)]
3. Yu, J.; Chen, K.; Azough, F.; Alvarez-Ruiz, D.T.; Reece, M.I.; Freer, R. Enhancing the thermoelectric performance of calcium cobaltite ceramics by tuning composition and processing. *ACS Appl. Mater. Interfaces* **2020**, *12*, 47634–47646. [[CrossRef](#)] [[PubMed](#)]
4. Zhang, W.; Zhu, K.; Liu, J.; Wang, J.; Yan, K.; Liu, P.; Wang, Y. Influence of the phase transformation in  $\text{Na}_x\text{CoO}_2$  ceramics on thermoelectric properties. *Ceram. Int.* **2018**, *44*, 17251–17257. [[CrossRef](#)]
5. Li, Z.; Xiao, C.; Xie, Y. Layered thermoelectric materials: Structure, bonding, and performance mechanisms. *Appl. Phys. Rev.* **2020**, *9*, 011303. [[CrossRef](#)]
6. Kuzanyan, A.S.; Margani, N.G.; Zhghamadze, V.V.; Mumladze, G.; Badalyan, G.R. Impact of  $\text{Sr}(\text{BO}_2)_2$  Dopant on Power Factor of  $\text{Bi}_2\text{Sr}_2\text{Co}_{1.8}\text{O}_y$  Thermoelectric. *J. Contemp. Phys.* **2021**, *56*, 146–149. [[CrossRef](#)]
7. Oopathumpa, C.; Boonthuma, D.; Smith, S.M. Effect of Poly(Vinyl Alcohol) on Thermoelectric Properties of Sodium Cobalt Oxide. *Key Eng. Mater.* **2019**, *798*, 304–309. [[CrossRef](#)]
8. Mallick, M.M.; Vitta, V. Enhancing Thermoelectric Figure-of-Merit of Polycrystalline  $\text{Na}_y\text{CoO}_2$  by a Combination of Non-stoichiometry and Co-substitution. *J. Electron. Mater.* **2018**, *47*, 3230–3237. [[CrossRef](#)]
9. Yu, J.; Chang, Y.; Jakubczyk, E.; Wang, B.; Azough, F.; Dorey, R.; Freer, R. Modulation of electrical transport in calcium cobaltite ceramics and thick films through microstructure control and doping. *J. Eur. Ceram. Soc.* **2021**, *41*, 4859–4869. [[CrossRef](#)]
10. Noudem, J.G.; Xing, Y. Overview of Spark Plasma Texturing of Functional Ceramics. *Ceramics* **2021**, *4*, 97–107. [[CrossRef](#)]
11. Jansen, M.; Hoppe, R. Notiz zur Kenntnis der Oxocobaltate des Natriums. *Z. Für Anorg. Und Allg. Chem.* **1974**, *408*, 104–106. [[CrossRef](#)]
12. Terasaki, I.; Sasago, Y.; Uchinokura, K. Large thermoelectric power in  $\text{NaCo}_2\text{O}_4$  single crystals. *Phys. Rev. B* **1997**, *56*, R12685–R12687. [[CrossRef](#)]
13. Koumoto, K.; Terasaki, I.; Funahashi, R. Complex Oxide Materials for Potential Thermoelectric Applications. *MRS Bull.* **2006**, *31*, 206–210. [[CrossRef](#)]
14. Viciu, L.; Huang, Q.; Cava, R.J. Stoichiometric oxygen content in  $\text{Na}_x\text{CoO}_2$ . *Phys. Rev. B* **2006**, *73*, 212107. [[CrossRef](#)]
15. Han, Y.; Ruan, Y.; Xue, M.; Shi, M.; Song, Z.; Zhou, Y.; Teng, J. Effect of Annealing Time on the Cyclic Characteristics of Ceramic Oxide Thin Film Thermocouples. *Micromachines* **2022**, *13*, 1970. [[CrossRef](#)]
16. Krasutskaya, N.S.; Klyndyuk, A.I.; Evseeva, L.E.; Gundilovich, N.N.; Chizova, E.A.; Paspelau, A.V. Enhanced thermoelectric performance of  $\text{Na}_{0.55}\text{CoO}_2$  ceramics doped by transition and heavy metal oxides. *Solids* **2024**, *5*, 267–277. [[CrossRef](#)]
17. Molenda, J.; Baster, D.; Milewska, A.; Świerczek, K.; Bora, D.K.; Braun, A.; Tobola, J. Electronic origin of difference in discharge curve between  $\text{Li}_x\text{CoO}_2$  and  $\text{Na}_x\text{CoO}_2$  cathodes. *Solid State Ion.* **2014**, *271*, 15–27. [[CrossRef](#)]
18. Pohle, B.; Gorbunov, M.; Lu, Q.; Bahrami, A.; Nielsch, K.; Mikhailova, D. Structural and electrochemical properties of layered  $\text{P2-Na}_{0.8}\text{Co}_{0.8}\text{Ti}_{0.2}\text{O}_2$  cathode in sodium-ion batteries. *Energies* **2022**, *15*, 3371. [[CrossRef](#)]

19. Nguyen, L.M.; Nguyen, V.H.; Nguyen, D.M.N.; Le, M.K.; Tran, V.M.; Le, M.L.P. Evaluating electrochemical properties of layered  $\text{Na}_x\text{Mn}_{0.5}\text{Co}_{0.5}\text{O}_2$  obtained at different calcined temperatures. *Chemengineering* **2023**, *7*, 33. [[CrossRef](#)]
20. Baster, D.; Zając, W.; Kondracki, Ł.; Hartman, F.; Molenda, J. Improvement of electrochemical performance of  $\text{Na}_{0.7}\text{Co}_{1-y}\text{Mn}_y\text{O}_2$ -cathode material for rechargeable sodium-ion batteries. *Solid State Ion.* **2016**, *288*, 213–218. [[CrossRef](#)]
21. Banobre-López, M.; Rivadulla, F.; Caudillo, R.; López-Quintela, M.A.; Rivas, J.; Goodenough, J.B. Role of doping and Dimensionality in the Superconductivity of  $\text{Na}_x\text{CoO}_2$ . *Chem. Mater.* **2005**, *17*, 1965–1968. [[CrossRef](#)]
22. Akram, R.; Khan, J.; Rafique, S.; Hussain, M.; Maqsood, A.; Naz, A.A. Enhanced thermoelectric properties of single phase Na doped  $\text{Na}_x\text{CoO}_2$  thermoelectric material. *Mater. Lett.* **2021**, *300*, 130180. [[CrossRef](#)]
23. Assadi, M.H.N.; Katayama-Yoshida, H. Restoration of long range order of Na ions in  $\text{Na}_x\text{CoO}_2$  at high temperatures by sodium site doping. *Comput. Mater. Sci.* **2015**, *109*, 308–311. [[CrossRef](#)]
24. Lee, M.; Viciu, L.; Li, L.; Wang, Y.; Foo, M.L.; Watauchi, S.; Pascal, R.A., Jr.; Cava, R.J.; Ong, N.P. Enhancement of thermopower in  $\text{Na}_x\text{CoO}_2$  in the large-x regime ( $x \geq 0.75$ ). *Phys. B* **2008**, *403*, 1564–1568. [[CrossRef](#)]
25. Krasutskaya, N.S.; Klyndyuk, A.I.; Evseeva, L.E.; Tanaeva, S.A. Synthesis and properties of  $\text{Na}_x\text{CoO}_2$  ( $x = 0.55, 0.89$ ) oxide thermoelectric. *Inorg. Mater.* **2016**, *52*, 393–399. [[CrossRef](#)]
26. Plewa, A.; Kulka, A.; Kondracki, Ł.; Lu, L.; Molenda, J. Phase diagram of  $\text{NaFe}_y\text{Co}_{1-y}\text{O}_2$  and evolution of its physico- and electrochemical properties with changing iron content. *J. Power Sources* **2019**, *419*, 42–51. [[CrossRef](#)]
27. Devi Meena, J.; Gayathri, N.; Bharathi, A.; Ramachandran, K. Effect of nickel substitution on thermal properties of  $\text{Na}_{0.9}\text{CoO}_2$ . *Bull. Mater. Sci.* **2007**, *30*, 345–348. [[CrossRef](#)]
28. Zhou, R.; Li, J.; Wei, W.; Li, X.; Luo, M. Atomic substituents effect on boosting desalination performances of Zn-doped  $\text{Na}_x\text{CoO}_2$ . *Desalination* **2020**, *496*, 114695. [[CrossRef](#)]
29. Ono, Y.; Kato, N.; Miyazaki, Y.; Kajitani, T. Transport Properties of Ca-doped  $\gamma\text{-Na}_x\text{CoO}_2$ . *J. Ceram. Soc. Jpn.* **2004**, *5*, S626–S628. [[CrossRef](#)]
30. Bos, J.W.G.; Hertz, J.T.; Morosan, E.; Cava, R.J. Magnetic and thermoelectric properties of layered  $\text{Li}_x\text{Na}_y\text{CoO}_2$ . *J. Chemistry State Chem.* **2007**, *180*, 3211–3217. [[CrossRef](#)]
31. Yang, X.; Wang, X.; Liu, J.; Hu, Z. Power factor enhancement in  $\text{Na}_x\text{CoO}_2$  doped by Bi. *J. Alloys Compd.* **2014**, *582*, 59–63. [[CrossRef](#)]
32. Seetawan, T.; Amornkitbambur, V.; Burinprakhon, T.; Maensiri, S.; Kurosaki, K.; Muta, H.; Uno, M.; Yamanaka, S. Thermoelectric power and electrical resistivity of Ag-doped  $\text{Na}_{1.5}\text{Co}_2\text{O}_4$ . *J. Alloys Compd.* **2006**, *407*, 314–317. [[CrossRef](#)]
33. Hussein, M.; Assadi, N. Hf doping for enhancing the thermoelectric performance in layered  $\text{Na}_{0.75}\text{CoO}_2$ . *Mater. Today Proc.* **2021**, *42*, 1542–1546. [[CrossRef](#)]
34. Nakhwong, R. Effect of reduced graphene oxide on the enhancement of thermoelectric power factor of  $\gamma\text{-Na}_x\text{Co}_2\text{O}_4$ . *Mater. Sci. Eng. B* **2020**, *261*, 114679. [[CrossRef](#)]
35. Ito, M.; Nagira, T.; Furumoto, D.; Katsuyama, S.; Nagai, H. Synthesis of  $\text{Na}_x\text{CoO}_2$  thermoelectric oxides by the polymerized complex method. *Scr. Mater.* **2003**, *48*, 403–408. [[CrossRef](#)]
36. Suan, M.S.M.; Farhan, M.A.; Lau, K.T.; Munawar, R.F.; Ismail, S. Structural and Electrical Properties of  $\text{Na}_x\text{CoO}_2$  Thermoelectric Synthesized via Citric-Nitrate Auto-Combustion Reaction. *J. Phys. Conf. Ser.* **2018**, *1082*, 012033. [[CrossRef](#)]
37. Itahara, H.; Fujita, K.; Sugiyama, J.; Nakamura, K.; Tani, T. Highly Textured  $\text{Na}_x\text{CoO}_2$ - $\delta$  Ceramics Fabricated by Both Templated Grain Growth and Reactive Templated Grain Growth Methods Using Single-Crystalline Particles as Templates. *J. Ceram. Soc. Jpn.* **2003**, *111*, 227–231. [[CrossRef](#)]
38. Park, K.; Jang, K.U.; Know, H.-C.; Kim, J.-G.; Cho, W.-S.Y. Influence of partial substitution of Cu for Co on the thermoelectric properties of  $\text{NaCo}_2\text{O}_4$ . *J. Alloys Compd.* **2006**, *419*, 213–219. [[CrossRef](#)]
39. Terasaki, I.; Tsukada, I.; Iguchi, Y. Impurity-induced transition and impurity-enhanced thermopower in the thermoelectric oxide  $\text{NaCo}_{2-x}\text{Cu}_x\text{O}_4$ . *Phys. Rev. B* **2002**, *65*, 195106. [[CrossRef](#)]
40. Park, K.; Choi, J.W.; Lee, G.W.; Kim, S.-J.; Lim, Y.-S.; Choi, S.-M.; Seo, W.-S.; Lim, S.M. Thermoelectric Properties of Solution-Combustion-Processed  $\text{Na}(\text{Co}_{1-x}\text{Ni}_x)_2\text{O}_4$ . *Mater. Lett.* **2012**, *18*, 1061–1065. [[CrossRef](#)]
41. Park, K.; Jang, K.U. Improvement in High-Temperature Properties of  $\text{NaCo}_2\text{O}_4$  through Partial Substitution of Ni for Co. *Mater. Lett.* **2006**, *60*, 1106–1110. [[CrossRef](#)]
42. Park, K.; Lee, J.H. Enhanced Thermoelectric Properties of  $\text{NaCo}_2\text{O}_4$  by Adding Zn. *Mater. Lett.* **2008**, *62*, 2366–2368. [[CrossRef](#)]
43. Tian, Z.; Wang, X.; Liu, J.; Lin, Z.; Hu, Y.; Wu, Y.; Han, C.; Hu, Z. Power factor enhancement induced by Bi and Mn co-substitution in  $\text{Na}_x\text{CoO}_2$  thermoelectric materials. *J. Alloys Compd.* **2016**, *661*, 161–167. [[CrossRef](#)]
44. Shin, W.; Murayama, N.; Ikeda, K.; Sago, S.; Terasaki, I. Thermoelectric Device of  $\text{Na}(\text{Co,Cu})_2\text{O}_4$  and  $(\text{Ba,Sr})\text{PbO}_3$ . *J. Ceram. Soc. Jpn.* **2002**, *110*, 727–730. [[CrossRef](#)]
45. Klyndyuk, A.I.; Krasutskaya, N.S.; Chizhova, E.A.; Evseeva, L.E.; Tanaeva, S.A. Synthesis and properties of  $\text{Na}_{0.55}\text{Co}_{0.9}\text{M}_{0.1}\text{O}_2$  ( $M = \text{Sc, Ti, Cr-Zn, Mo, W, Pb, Bi}$ ) solid solutions. *Glass Phys. Chem.* **2016**, *42*, 100–107. [[CrossRef](#)]

46. Shannon, D.; Prewitt, C.T. Effective ionic radii in oxides and fluorides, Acta Crystallographica Section B: Structural Science. *Cryst. Eng. Mater.* **1969**, *25*, 925–946.
47. Greenstein, G.R. The Merck index: An Encyclopedia of Chemicals, Drugs, and Biologicals. *Ref. Rev.* **2025**, *21*, 2746.
48. Klyndyuk, A.I.; Krasutskaya, N.S.; Dyatlova, E.M. Influence of sintering temperature on the properties of  $\text{Na}_x\text{CoO}_2$  ceramics. *Proc. BSTU* **2010**, *XVIII*, 99–102. (In Russian)
49. Pyatnitsky, I.V. *Analytical Chemistry of Cobalt*; Science: Moscow, Russia, 1965; 292p. (In Russian)
50. Sopicka-Lizer, M.; Kozłowska, K.; Bobrowska-Grzesik, E.; Plewa, J.; Altenburg, H. Assessment of Co(II), Co(III) and Co(IV) content in thermoelectric cobaltites. *Arh. Metall. Mater.* **2009**, *54*, 881–888.
51. Azad, S.; Kumar, N.; Chand, S. Structural, morphological, optical and dielectric properties of  $\text{Ti}_{1-x}\text{Fe}_x\text{O}_2$  nanoparticles synthesized using sol-gel method. *J. Sol-Gel Sci. Technol.* **2022**, *105*, 163–175. [[CrossRef](#)]
52. Marwah, T.J. Using the size strain plot method to specify lattice parameters. *Haitham J. Pure Appl. Sci.* **2023**, *36*, 123–129. [[CrossRef](#)]
53. Lotgering, F.K. Topotactical reactions with ferrimagnetic oxides having hexagonal crystal structures. *J. Inorg. Nucl. Chem.* **1959**, *9*, 113–123. [[CrossRef](#)]
54. Klyndyuk, A.I.; Chizhova, E.A.; Latypov, R.S.; Shevchenko, S.V.; Kononovich, V.M. Effect of the addition of copper particles on the thermoelectric properties of the  $\text{Ca}_3\text{Co}_4\text{O}_{9+\delta}$  ceramics produced by two-step sintering. *Inorg. Mater.* **2022**, *67*, 237–244. [[CrossRef](#)]
55. Klyndyuk, A.I.; Petrov, G.S.; Poluyan, A.F.; Bashkirov, L.A. Structure and Physicochemical Properties of  $\text{Y}_2\text{Ba}_{1-x}\text{M}_x\text{CuO}_5$  ( $M = \text{Sr}, \text{Ca}$ ) Solid Solutions. *Inorg. Mater.* **1999**, *35*, 512–516. [[CrossRef](#)]
56. Zorkovská, A.; Feher, A.; Sébek, J.; Šantavá, E.; Bradaric, I. Non-Fermi-liquid behavior in the layered  $\text{Na}_x\text{CoO}_2$ . *Low Temp. Phys.* **2007**, *33*, 944–947. [[CrossRef](#)]
57. Snyder, G.J.; Ursell, T.S. Thermoelectric Efficiency and Compatibility. *Phys. Rev. Lett.* **2003**, *91*, 148301. [[CrossRef](#)]
58. Delmas, C.; Braconnier, J.-J.; Fouassier, C.; Hagenmuller, P. Electrochemical intercalation of sodium in  $\text{Na}_x\text{CoO}_2$  bronzes. *Solid State Ion.* **1981**, *3*, 165–169. [[CrossRef](#)]
59. Liu, P.; Chen, G.; Cui, Y.; Zhang, H.; Xiao, F.; Wang, L.; Nakano, H. High temperature electrical conductivity and thermoelectric power of  $\text{Na}_x\text{CoO}_2$ . *Solid State Ion.* **2008**, *179*, 2308–2312. [[CrossRef](#)]
60. Matsubara, I.; Zhou, Y.; Takeuchi, T.; Funahashi, R.; Shikano, M.; Murayama, N.; Shin, W.; Izu, N. Thermoelectric properties of spark-plasma-sintered  $\text{Na}_{1+x}\text{Co}_2\text{O}_4$  ceramics. *J. Ceramic. Soc. Jpn.* **2003**, *111*, 238–241. [[CrossRef](#)]
61. Li, N.; Jiang, Y.; Li, G.; Wang, C.; Shi, J.; Yu, D. Self-ignition route to Ag-doped  $\text{Na}_{1.7}\text{Co}_2\text{O}_4$  and its thermoelectric properties. *J. Alloys Compd.* **2009**, *467*, 444–449. [[CrossRef](#)]
62. Lei, Y.; Li, X.; Liu, L.; Ceder, G. Synthesis and Stoichiometry of Different Layered Sodium Cobalt Oxides. *Chem. Mater.* **2014**, *26*, 5288–5296. [[CrossRef](#)]
63. Klyndyuk, A.I.; Matsukevich, I.V. Synthesis, structure and properties of  $\text{Ca}_3\text{Co}_{3.85}\text{M}_{0.15}\text{O}_{9+\delta}$  ( $M = \text{Ti-Zn}, \text{Mo}, \text{W}, \text{Pb}, \text{Bi}$ ). *Russ. J. Inorg. Chem.* **2015**, *51*, 1025–1031. [[CrossRef](#)]
64. Lin, Y.-H.; Lan, J.; Shen, Z.; Liu, Y.; Nan, C.-W.; Li, J.-F. High-temperature electrical transport behaviors in textured  $\text{Ca}_3\text{Co}_4\text{O}_9$ -based polycrystalline ceramics. *Appl. Phys. Lett.* **2009**, *94*, 072107. [[CrossRef](#)]
65. Pan, L.; Mitra, S.; Zhao, L.-D.; Shen, Y.; Wang, Y.; Fesel, C.; Berardan, D. The Role of Ionized Impurity Scattering on the Thermoelectric Performances of Rock Salt  $\text{AgPb}_m\text{SnSe}_{2+m}$ . *Adv. Funct. Mater.* **2016**, *26*, 5149–5157. [[CrossRef](#)]
66. Snyder, G.J.; Snyder, A.H.; Wood, M.; Gurunathan, R.; Snyder, B.H.; Niu, C. Weighted Mobility. *Adv. Mater.* **2020**, *32*, 2001537. [[CrossRef](#)] [[PubMed](#)]
67. Wang, S.; Chen, S.; Liu, F.; Yan, G.; Chen, J.; Li, H.; Wang, J.; Yu, W.; Fu, G. Laser-induced voltage effects in  $c$ -axis inclined  $\text{Na}_x\text{CoO}_2$  thin films. *Appl. Surf. Sci.* **2012**, *258*, 7330–7333. [[CrossRef](#)]
68. Liu, W.; Tang, X.; Sharp, J. Low-temperature solid state synthesis and thermoelectric properties of high-performance and low-cost Sb-doped  $\text{Mg}_2\text{Si}_{0.6}\text{Sn}_{0.4}$ . *J. Phys. D Appl. Phys.* **2010**, *43*, 085406. [[CrossRef](#)]
69. Fergus, J.W. Oxide material for high temperature thermoelectric energy conversion. *J. Eur. Ceram. Soc.* **2012**, *32*, 525–540. [[CrossRef](#)]
70. Królicka, A.K.; Piersa, M.; Mirowska, A.; Michalska, M. Effect of sol-gel and solid state synthesis techniques on structural, morphological and thermoelectric performances of  $\text{Ca}_3\text{Co}_4\text{O}_9$ . *Ceram. Int.* **2018**, *44*, 13736–13743. [[CrossRef](#)]
71. Klyndyuk, A.I.; Krasutskaya, N.S.; Khort, A.A. Synthesis and Properties of Ceramics Based on a Layered Bismuth Calcium Cobaltite. *Inorg. Mater.* **2018**, *54*, 509–514. [[CrossRef](#)]

**Disclaimer/Publisher's Note:** The statements, opinions and data contained in all publications are solely those of the individual author(s) and contributor(s) and not of MDPI and/or the editor(s). MDPI and/or the editor(s) disclaim responsibility for any injury to people or property resulting from any ideas, methods, instructions or products referred to in the content.